Supplemental Material for Spin-selective Aharonov-Casher caging in a topological quantum network

Amrita Mukherjee,[1] Rudolf A. Römer,[2] and Arunava Chakrabarti[3]

[1]*Department of Physics, University of Kalyani, Kalyani, West Bengal-741 235, India*

[2]*Department of Physics, University of Warwick, Coventry CV4 7AL, United Kingdom*

[3]*Department of Physics, Presidency University, 86/1 College Street, Kolkata, West Bengal - 700073, India*

(Dated: October 9, 2019)

I. DISPERSION FOR THE CLEAN CASE

We compute the spin-dependent energy dispersion $E(k)$ relation after writing the Hamiltonian of the system in k-space. The relations for a spin-half particle in the diamond lattice are $E = 0$ and $E = \pm\sqrt{4 + 2\cos k + \cos(k - 2\lambda) + \cos(k + 2\lambda)}$. These states are doubly degenerate due to two spin projections of for a spin-half particle. The result is shown in Fig. S1.

II. PERIODIC BOUNDARIES

For the case of extreme localization at $\lambda = \pi/2$, there are only flat bands at $E = 0$ (Green) and ± 2 (Red) for the periodic array. The edge states have vanished, while at $\lambda = \pi/2$ we still observe flat bands as shown in Fig. S2.

III. ROBUSTNESS OF THE EDGE STATES

In Fig. S3(a), we show the resilience of our results when perturbed by a small additional disorder in the hopping strengths. Although the degeneracy of the edge states around $\lambda = -\pi, 0, \pi$ is lifted, the overall character of the edge states remains similar. Indeed, even more flat bands emerge at $\lambda = \pi/2$. In Fig. S3(b), we find that a small in-plane electric field also does not change the structure of the spectrum. Nevertheless, the exact degeneracy at $E = \pm 2$ for $\lambda = \pi/2$ is retained, suggesting a cancellation of terms at least to 1st order perturbation theory.

IV. DETAILS OF THE SPECTRUM AROUND SO COUPLING $\lambda = \pi/2$

Fig. 2 in the main text is quite busy, showing results for $s = 1/2, 1, 3/2$ and 2. In order to allow the reader to see the precise collapse of the spectrum at $\lambda = \pi/2$, Fig. S4 shows a close-up for hard wall and periodic boundaries. We note that the flat bands of edge states only appears in the hard-wall case. For a hopping disordered chain, cp. Fig. S4(c), the crossing point looses much of its focus while a system with an out-of-plane component, cp. Fig. S4(d), sees a small spreading of energy values around $E = \pm 2$. In both cases the states at $E = \pm\sqrt{2}$ are retained.

V. HOPPING INTEGRALS IN MATRIX FORM

The nearest-neighbor hopping matrices $\mathbf{t}_{xx'}$, leading to the renormalized hopping matrix as discussed in the main text, are given as follows. For the case $s = 1/2$, we have

$$\frac{t_x}{t} \equiv e^{i\lambda\sigma_x} = \begin{pmatrix} \cos\lambda & i\sin\lambda \\ i\sin\lambda & \cos\lambda \end{pmatrix}, \tag{S1a}$$

$$\frac{t_y}{t} \equiv e^{i\lambda\sigma_y} = \begin{pmatrix} \cos\lambda & \sin\lambda \\ -\sin\lambda & \cos\lambda \end{pmatrix}, \tag{S1b}$$

while for $s = 1$, we find

$$\frac{t_x}{t} \equiv e^{i\lambda\sigma_x} = \tag{S2a}$$
$$\begin{pmatrix} \cos^2\lambda & i\sqrt{2}\cos\lambda\sin\lambda & -\sin^2\lambda \\ i\sqrt{2}\cos\lambda\sin\lambda & \cos 2\lambda & i\sqrt{2}\cos\lambda\sin\lambda \\ -\sin^2\lambda & i\sqrt{2}\cos\lambda\sin\lambda & \cos^2\lambda \end{pmatrix},$$

$$\frac{t_y}{t} \equiv e^{i\lambda\sigma_y} = \tag{S2b}$$
$$\begin{pmatrix} \cos^2\lambda & \sqrt{2}\cos\lambda\sin\lambda & \sin^2\lambda \\ -\sqrt{2}\cos\lambda\sin\lambda & \cos 2\lambda & \sqrt{2}\cos\lambda\sin\lambda \\ \sin^2\lambda & -\sqrt{2}\cos\lambda\sin\lambda & \cos^2\lambda \end{pmatrix}.$$

At $\lambda = \pi/2$, all these $(2s+1) \times (2s+1)$ matrices reduce to an anti-diagonal structure. Hence, only paired $m_s = \pm n$ spin projections, with $n = 1/2, 1, \ldots s \geq 1$, are coupled while the $m_s = 0$ projection for half-odd integer s remains unpaired. This leads to the different transport characteristics as explained in the main text.

VI. TRANSPORT

The $\mathcal{T}_{m_s' m_s}$ defined in the main text combine as $T_{m_s} = \sum_{m_s' \neq m_s} \mathcal{T}_{m_s' m_s}$ to give the total spin transport for the m_s projection coming from the other possible projections for given s. It is these T_{m_s} which are plotted in Figs. 3+5 in the main text. See also Ref. 1.

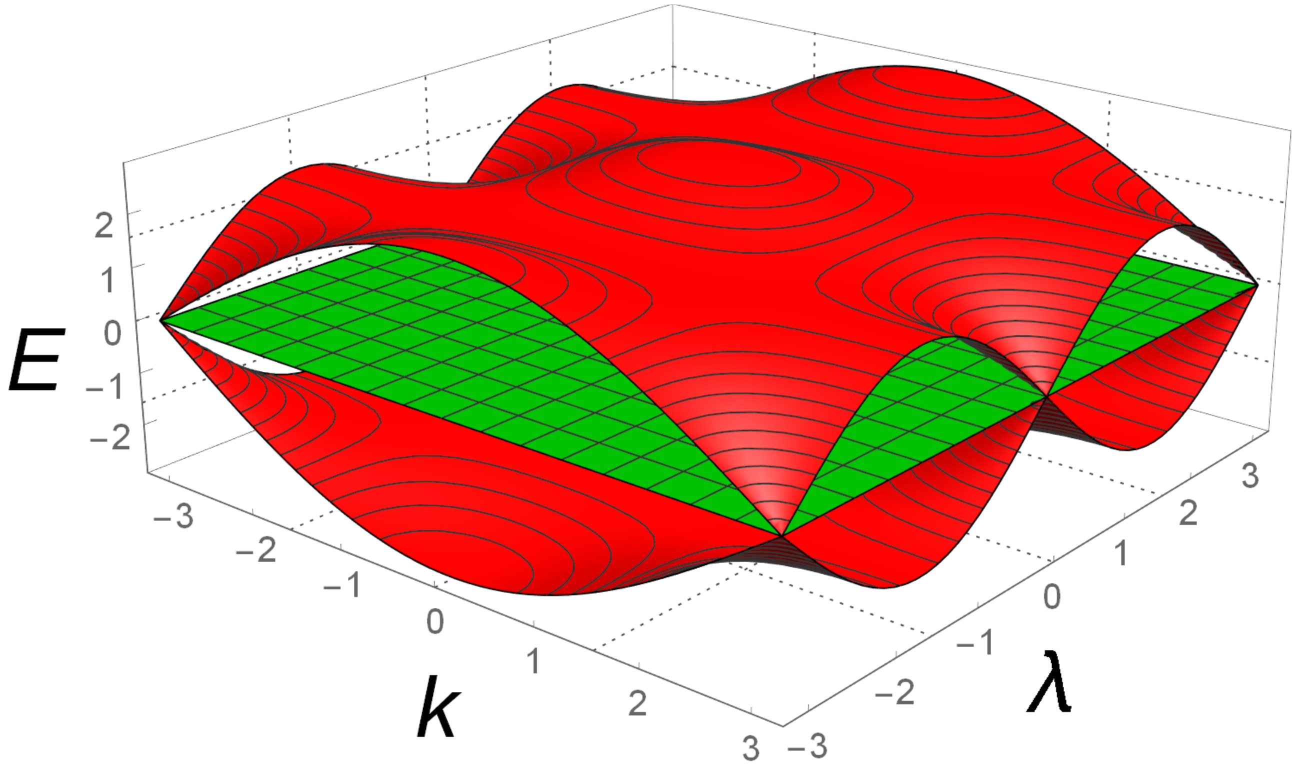

FIG. S1. Energy dispersion relation $E(k)$ for a periodic array of rhombi with $s = 1/2$ and varying SO strength λ. We note that the three visible sheets are doubly degenerate. The dashed grid lines indicate multiples of $\pi/2$ for both k and λ.

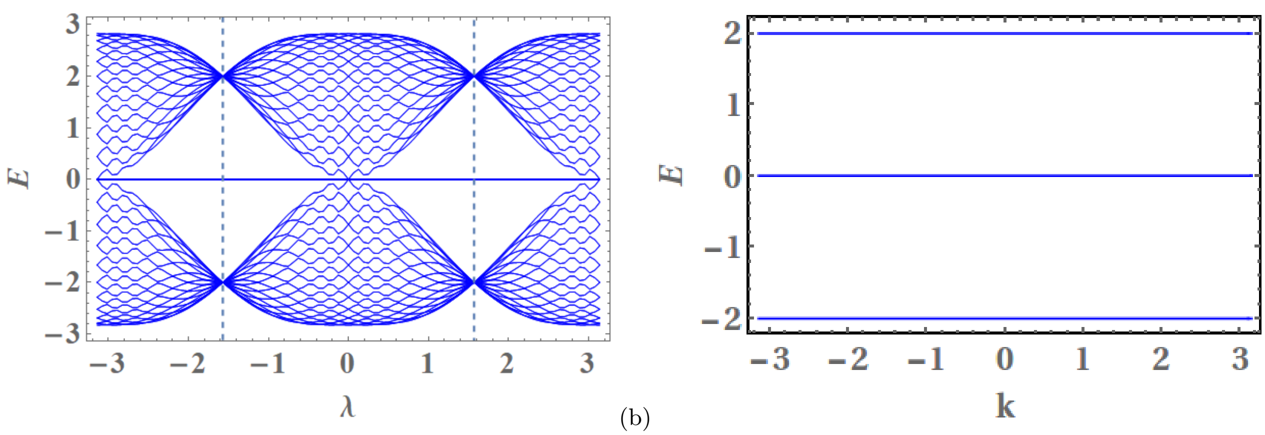

(a) (b)

FIG. S2. (a) Variation of eigenstates against the SO coupling λ (in units of t) for a 20-loop *periodic* rhombic array with $\epsilon = 0$ and $t = 1$ and spin $s = 1/2$. A flat, λ-independent band is seen at $E = 0$, and it is there for all spins. The vertical dashed lines highlight $\lambda = \pm\pi/2$. (b) The flat bands at $\lambda = \pi/2$ in the periodic case as a function of k.

SUPPLEMENTARY REFERENCE

[1] A. Mukherjee, A. Chakrabarti, and R. A. Römer, Phys. Rev. B. **98**, 075415 (2018).

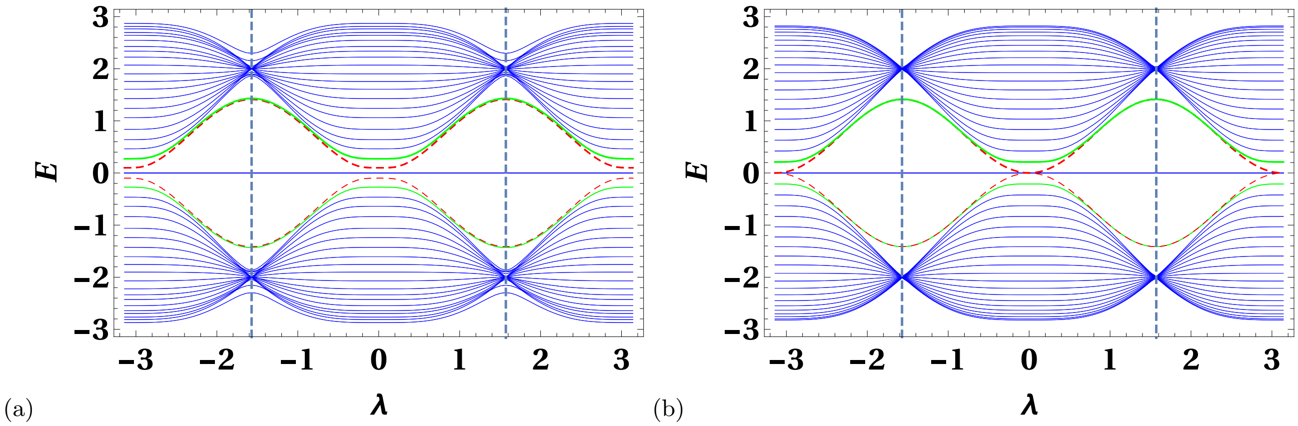

FIG. S3. (a) Energy spectrum for hopping disorder $t \in [0.75, 1.5]$. Result for a frozen-in disorder distribution is shown as an example. Colours as in the Fig. 2 of the main text. (b) Same for a small in-plane electric field $E_x = E_y = 0.1\lambda, E_z = \lambda$.

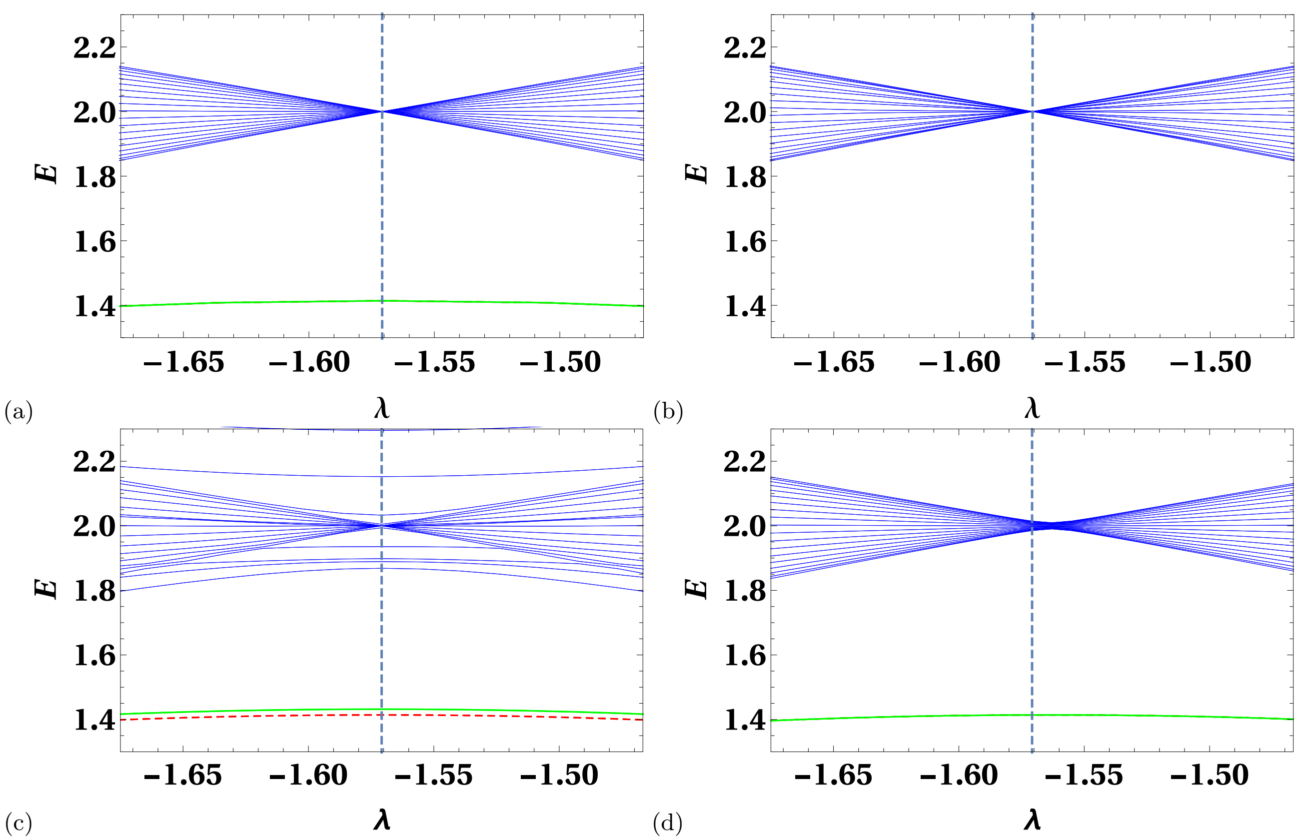

FIG. S4. Close-up details of the behaviour at $\lambda = \pi/2$ for (a) hard wall and (b) periodic systems. We note the clear reduction to a single point at $\lambda = \pi/2$ for 5 (± 2, $\pm\sqrt{2}$ and 0) or 3 (± 2, 0) energy values for the hard wall and periodic boundaries, respectively. Only the positive part of the spectrum $E \geq 1.35$ has been shown. (c) Same for hopping disorder $t \in [0.75, 1.5]$ with hard boundaries. (d) Results for a small in-plane electric field $E_x = E_y = 0.1\lambda, E_z = \lambda$ with hard boundaries. The color coding of the lines is as in Fig. 2 of the main text.